DALTON
FULL PAPER

Synthesis, structure and reactivity of triosmium clusters derived from the reactions of $[Os_3(CO)_{10}(\mu\text{-dppm})]$ (dppm = $Ph_2PCH_2PPh_2$) and $[Os_3(\mu\text{-H})(CO)_8\{Ph_2PCH_2P(Ph)C_6H_4\}]$ with $PHPh_2$

Kazi A. Azam,*[a] Michael B. Hursthouse,*[,†,b] Md. Rafiqul Islam,[a] Shariff E. Kabir,[c] K. M. Abdul Malik,[b] Rashid Miah,[a] Claas Sudbrake[c] and Heinrich Vahrenkamp*[,c]

[a] *Department of Chemistry, Jahangirnagar University, Savar, Dhaka-1342, Bangladesh*
[b] *Department of Chemistry, University of Wales Cardiff, P.O. Box 912, Park Place, Cardiff, UK CF1 3TB*
[c] *Institut für Anorganische und Analytische Chemie, Universität Freiburg, Alberstrasse 21, D-79104, Freiburg, Germany*

The reaction of $[Os_3(CO)_{10}(\mu\text{-dppm})]$ **1** with diphenylphosphine in refluxing toluene led to the substituted cluster $[Os_3(CO)_9(\mu\text{-dppm})(PHPh_2)]$ **3** and the phosphido-bridged dihydride $[Os_3H(\mu\text{-H})(CO)_7(\mu\text{-dppm})(\mu\text{-}PPh_2)_2]$ **4**. The cluster **4** exists as three isomeric forms in solution. The 46-electron compound $[Os_3(\mu\text{-H})(CO)_8\{Ph_2PCH_2P(Ph)C_6H_4\}]$ **2** reacted with an excess of $PHPh_2$ at room temperature to yield $[Os_3(\mu\text{-H})(CO)_8\{Ph_2PCH_2P(Ph)C_6H_4\}(PHPh_2)]$ **5** and $[Os_3(CO)_8(\mu\text{-dppm})(PHPh_2)_2]$ **6** in 16 and 62% yields respectively. Thermolysis of **6** in refluxing toluene gave **4** and two stereoisomeric compounds **7** and **8** with stoichiometry $[Os_3(\mu\text{-H})_2(CO)_6(\mu\text{-dppm})(\mu\text{-}PPh_2)_2]$. The cluster **3** decarbonylated at 110 °C to give the phosphido-bridged monohydride cluster $[Os_3(\mu\text{-H})(CO)_8(\mu\text{-dppm})(\mu\text{-}PPh_2)]$ **9** which exists as two isomers in solution. Compound **4** converts into **7** and **8** on thermolysis in toluene. All the compounds have been characterized by infrared, ^1H and $^{31}P\text{-}\{^1H\}$ NMR spectroscopy and elemental analysis and in the case of **3**, **4**, **6** and **7** also by X-ray crystallography.

The synthesis and reactivity of triosmium clusters containing bridging diphosphine ligands $[Os_3(CO)_{10}\{\mu\text{-}Ph_2P(CH_2)_nPPh_2\}]$ (n = 1–5) have widely been studied during the last decade.[1–14] In particular, the dppm [= bis(diphenylphosphino)methane, $Ph_2PCH_2PPh_2$] compound $[Os_3(CO)_{10}(\mu\text{-dppm})]$ **1** has attracted considerable attention because of its novel reactivity to give many interesting species and also because of the special ability of dppm to maintain the metal cluster framework intact during chemical reactions.[3–14] For example, decarbonylation of **1** in refluxing toluene gives the co-ordinatively unsaturated cluster $[Os_3(\mu\text{-H})(CO)_8\{Ph_2PCH_2P(Ph)C_6H_4\}]$ **2** which reacts with CO to form $[Os_3(\mu\text{-H})(CO)_9\{Ph_2PCH_2(Ph)C_6H_4\}]$,[7] with H_2 to form $[Os_3(\mu\text{-H})_2(CO)_8(\mu\text{-dppm})]$,[8] with diphenylacetylene to form $[Os_3(CO)_8(\mu\text{-dppm})(PhC{\equiv}CPh)]$[9] and with $[Au(PPh_3)]PF_6$ and HBF_4 to form the cationic clusters $[Os_3(\mu\text{-H})(CO)_8\{Ph_2PCH_2P(Ph)C_6H_4\}(\mu\text{-}AuPPh_3)]PF_6$ and $[Os_3(\mu\text{-H})_2(CO)_8\{Ph_2PCH_2P(Ph)C_6H_4\}]BF_4$ respectively.[10]

Another aspect of the reactivity of compound **1** or its acetonitrile derivative $[Os_3(CO)_9(\mu\text{-dppm})(MeCN)]$ is the derivative chemistry with monodentate phosphines L to give $[Os_3(CO)_9(\mu\text{-dppm})L]$ [L = PPh_3, $P(OMe)_3$ or $Ph_2PCH_2CH_2Si(OEt)_3$] and with bidentate dppm to give $[Os_3(CO)_9(\mu\text{-dppm})(\text{dppm-}P)]$ and $[Os_3(CO)_8(\mu\text{-dppm})_2]$.[4,5,12,13] The bis-phosphine or -phosphite derivatives $[Os_3(CO)_8(\mu\text{-dppm})(PPh_3)_2]$ or $[Os_3(CO)_8(\mu\text{-dppm})\{P(OMe)_3\}_2]$ are also formed by the reaction of **2** with PPh_3 or $P(OMe)_3$ by demetallation of the phenyl group of the diphosphine ligand.[11] In an earlier study we[14] investigated the oxidative-addition reaction of PhSH to **1** to yield $[Os_3(\mu\text{-H})(CO)_8(\mu\text{-SPh})(\mu\text{-dppm})]$ while Lewis and co-workers[5] reported similar compounds by the reaction of RSH (R = Ph or Et) with $[Os_3(CO)_9(\mu\text{-dppm})(MeCN)]$ (Scheme 1).

In recent years there has been increasing interest in phosphido-bridged di- and poly-nuclear transition-metal hydride complexes mainly due to their low tendency to fragment into monometallic species and consequently to their potential use in many stoichiometric and catalytic reactions.[15–17] Trinuclear complexes of the iron triad containing bridging phosphide and hydride ligands have been reported from the oxidative addition of P–H bonds in primary or secondary phosphines to the metal carbonyls.[18–21] For example, the synthesis of $[Fe_3(\mu\text{-H})_2(CO)_8(\mu\text{-}PPh_2)_2]$ has previously been reported[20] in very low yield (1%) from the reaction of $[Fe_3(CO)_{12}]$ with $PHPh_2$. Haines and co-workers[21] reported the corresponding ruthenium analogue $[Ru_3(\mu\text{-H})_2(CO)_8(\mu\text{-}PPh_2)_2]$ from the reaction of $PHPh_2$ with $[Ru_3(CO)_{12}]$. A shortcoming of this method is that thermal or photochemical activation needed to effect P–H bond cleavage may lead to fragmentation of the metal carbonyl precursor and low yields of the phosphido-bridged hydrido cluster. Mays and co-workers[18] described a series of trinuclear complexes containing PH_2Ph and/or capping PPh ligands from the thermal reaction of $[M_3(CO)_{12}]$ (M = Ru or Os) with PH_2Ph. Later Carty and co-workers[19] reported the phosphido-bridged dihydrido clusters $[M_3(\mu\text{-H})_2(CO)_8(\mu\text{-}PPh_2)_2]$ (M = Ru or Os) in moderate yield from the thermolysis of $[M_3(CO)_{10}(PHPh_2)_2]$ whereas the iron analogue $[Fe_3(\mu\text{-H})_2(CO)_8(\mu\text{-}PPh_2)_2]$ is obtained in 60% yield from the controlled degradation of $[Fe_4(\mu\text{-H})_2(CO)_{13}]$ with hydrogen elimination in the presence of $PHPh_2$. Carty and co-workers[22] also reported the highly reactive 46-electron cluster $[Ru_3(\mu\text{-H})(CO)_9(\mu\text{-}PPh_2)]$ from the Me_3NO-initiated decarbonylation of $[Ru_3(\mu\text{-H})(CO)_{10}(\mu\text{-}PPh_2)]$. The phosphido cluster $[Ru_3(\mu\text{-H})_2(CO)_6\{(\mu\text{-PPh})CH_2PPh_2\}_2]$ which is a hydrogenation catalyst containing two phosphido phosphine ligands has been

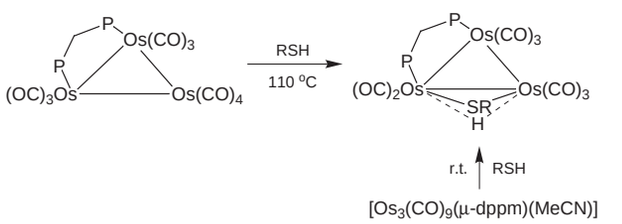

Scheme 1 r.t. = Room temperature

† E-Mail: hursthouse@cardiff.ac.uk

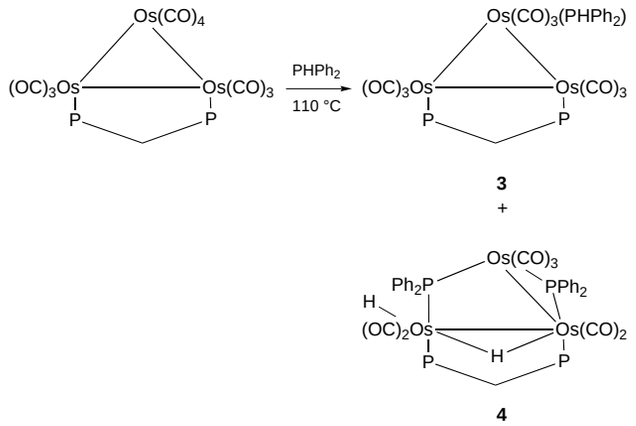

Scheme 2

reported[23] from the hydrogenation of $[Ru_3(CO)_8(\mu\text{-dppm})_2]$ at 85 °C.

Following our interest in this type of reactivity we have attempted the preparation of μ-phosphido complexes by direct thermal reaction of $PHPh_2$ with the dppm-bridged compound **1**. In the present paper we describe the synthesis, structure and decarbonylation reactions of $[Os_3(CO)_9(\mu\text{-dppm})(PHPh_2)]$, $[Os_3H(\mu\text{-H})(CO)_7(\mu\text{-dppm})(\mu\text{-}PPh_2)_2]$, $[Os_3(CO)_8(\mu\text{-dppm})(PHPh_2)_2]$ and $[Os_3(\mu\text{-H})_2(CO)_6(\mu\text{-dppm})(\mu\text{-}PPh_2)_2]$. We also demonstrate that $[Os_3H(\mu\text{-H})(CO)_7(\mu\text{-dppm})(\mu\text{-}PPh_2)_2]$ is formed *via* compound $[Os_3(CO)_8(\mu\text{-dppm})(PHPh_2)_2]$ which in turn is synthesized from the reaction of **2** with $PHPh_2$.

Results and Discussion

The cluster $[Os_3(CO)_{10}(\mu\text{-dppm})]$ **1** reacts with $PHPh_2$ at 110 °C to give $[Os_3(CO)_9(\mu\text{-dppm})(PHPh_2)]$ **3** and $[Os_3H(\mu\text{-H})(CO)_7(\mu\text{-dppm})(\mu\text{-}PPh_2)_2]$ **4** in 70 and 15% yields respectively (Scheme 2). Both compounds **3** and **4** were characterized by infrared, ^1H and $^{31}P\text{-}\{^1H\}$ spectroscopic data, elemental analysis and single-crystal structure determination. The infrared spectrum of **3** in the carbonyl stretching region is very similar to that of the PPh_3-substituted analogue $[Os_3(CO)_9(\mu\text{-dppm})(PPh_3)]$ which was reported from the reaction of PPh_3 with **1** at 110 °C[12] or with $[Os_3(CO)_9(\mu\text{-dppm})(MeCN)]$ at ambient temperature.[5] The ^1H NMR spectrum of **3** contains a triplet at δ 3.82 (J_{PH} = 10.4 Hz) due to the methylene protons of the dppm ligand, a doublet at δ 6.29 (J = 383.4 Hz) due to the P–H proton of the $PHPh_2$ ligand and a multliplet centered at δ 6.35 due to the phenyl protons of both the ligands. The magnitude of the phosphorus–hydrogen coupling constant of the doublet at δ 6.29 is similar to those reported for other trimetallic clusters containing terminal PH_2Ph and $PHPh_2$ moieties.[20] The $^{31}P\text{-}\{^1H\}$ NMR spectrum shows two doublets at δ 12.5 and 10.9 (J = 54.7 Hz) assigned to the phosphorus atom of the dppm ligand and a singlet at δ 38.8 assigned to the phosphorus atom of the $PHPh_2$ ligand. This is consistent with the structure where the dppm bridges two equatorial sites and the $PHPh_2$ ligand occupies an equatorial site on the unique osmium atom. The spectroscopic data, therefore, suggest that **3** has a structure similar to those of $[Os_3(CO)_9(\mu\text{-dppm})(PPh_3)]$,[5,12] $[Os_3(CO)_9(\mu\text{-dppm})\{P(OMe)_3\}]$[5] and $[Os_3(CO)_9(\mu\text{-dppm})(\text{dppm-}P)]$.[13]

In order to confirm the proposed structure of compound **3** a single-crystal X-ray study was carried out. The molecular structure is shown in Fig. 1 and selected bond distances and angles are summarized in Table 1. The structure is derived from $[Os_3(CO)_{12}]$[24] by replacement of one equatorial carbonyl group on each of the three osmium atoms by a bidentate dppm ligand and a monodentate $PHPh_2$ ligand in such a way that one Os–Os bond is bridged by the dppm ligand co-ordinated at equatorial sites while the $PHPh_2$ ligand is co-ordinated also at an equatorial site to the third osmium atom. The overall structure is similar to that of $[Os_3(CO)_9(\mu\text{-dppm})(\text{dppm-}P)]$.[13] The bridged

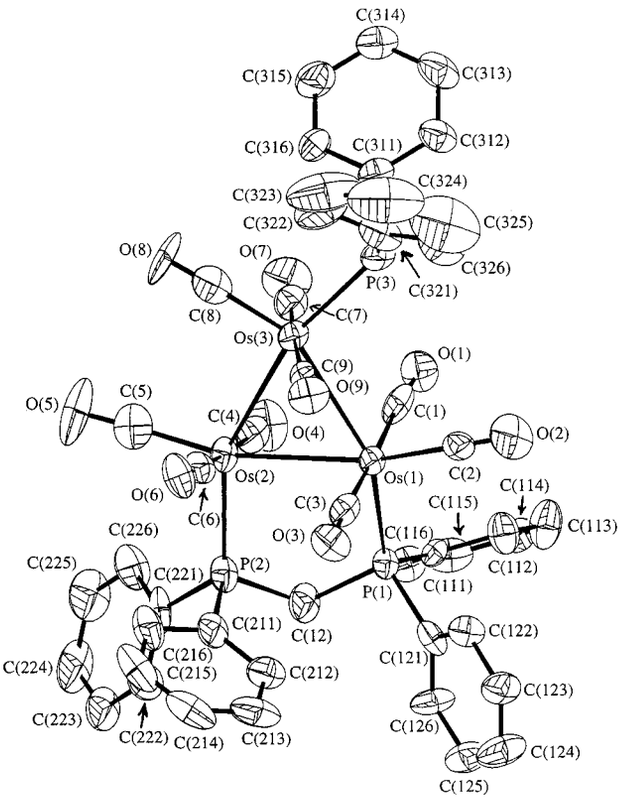

Fig. 1 Solid-state structure of $[Os_3(CO)_9(\mu\text{-dppm})(PHPh_2)]$ **3** showing the atom labelling scheme. Thermal ellipsoids are drawn at 35% probability level. The hydrogen atoms are omitted for clarity

Table 1 Selected bond lengths (Å) and angles (°) for $[Os_3(CO)_9(\mu\text{-dppm})(PHPh_2)]$ **3**

Os(1)–Os(3)	2.8790(8)	Os(1)–Os(2)	2.8805(7)
Os(2)–Os(3)	2.8604(8)	Os(1)–P(1)	2.338(3)
Os(2)–P(2)	2.317(3)	Os(3)–P(3)	2.325(3)
Os–C (CO)*	1.89	C–O*	1.18
C(1)–Os(1)–C(3)	175.6(5)	C(1)–Os(1)–C(2)	92.0(5)
C(3)–Os(1)–C(2)	87.0(5)	C(1)–Os(1)–P(1)	91.7(4)
C(3)–Os(1)–P(1)	92.7(3)	C(2)–Os(1)–P(1)	105.5(4)
C(1)–Os(1)–Os(3)	81.8(4)	C(3)–Os(1)–Os(3)	94.3(4)
C(2)–Os(1)–Os(3)	103.6(4)	P(1)–Os(1)–Os(3)	150.38(8)
C(1)–Os(1)–Os(2)	96.3(4)	C(3)–Os(1)–Os(2)	83.2(4)
C(2)–Os(1)–Os(2)	159.6(4)	P(1)–Os(1)–Os(2)	92.87(8)
Os(3)–Os(1)–Os(2)	59.56(2)	C(4)–Os(2)–C(5)	90.3(6)
C(4)–Os(2)–C(6)	174.8(5)	C(5)–Os(2)–C(6)	91.3(6)
C(4)–Os(2)–P(2)	91.7(4)	C(5)–Os(2)–P(2)	103.4(5)
C(6)–Os(2)–P(2)	92.8(4)	C(4)–Os(2)–Os(3)	94.2(4)
C(5)–Os(2)–Os(3)	107.7(5)	C(6)–Os(2)–Os(3)	80.6(4)
P(2)–Os(2)–Os(3)	148.31(9)	C(4)–Os(2)–Os(1)	82.7(4)
C(5)–Os(2)–Os(1)	165.2(5)	C(6)–Os(2)–Os(1)	94.6(4)
P(2)–Os(2)–Os(1)	89.85(9)	Os(3)–Os(2)–Os(1)	60.20(2)
C(7)–Os(3)–C(9)	174.5(5)	C(7)–Os(3)–C(8)	94.9(6)
C(9)–Os(3)–C(8)	90.6(5)	C(7)–Os(3)–P(3)	91.3(4)
C(9)–Os(3)–P(3)	88.4(4)	C(8)–Os(3)–P(3)	98.9(4)
C(7)–Os(3)–Os(2)	83.0(4)	C(9)–Os(3)–Os(2)	95.7(3)
C(8)–Os(3)–Os(2)	98.3(4)	P(3)–Os(3)–Os(2)	162.28(9)
C(7)–Os(3)–Os(1)	94.1(4)	C(9)–Os(3)–Os(1)	80.7(3)
C(8)–Os(3)–Os(1)	155.4(4)	P(3)–Os(3)–Os(1)	103.71(9)
Os(2)–Os(3)–Os(1)	60.25(2)	C(12)–P(1)–C(111)	103.3(5)
C(12)–P(1)–C(121)	103.3(6)	C(111)–P(1)–C(121)	101.0(4)
C(12)–P(1)–Os(1)	114.3(5)	C(111)–P(1)–Os(1)	114.2(3)
C(121)–P(1)–Os(1)	118.6(3)	C(211)–P(2)–C(221)	102.4(4)
C(211)–P(2)–C(12)	107.7(6)	C(221)–P(2)–C(12)	98.0(5)
C(211)–P(2)–Os(2)	115.5(3)	C(221)–P(2)–Os(2)	119.5(4)
C(12)–P(2)–Os(2)	111.9(4)	C(321)–P(3)–C(311)	102.2(5)
C(321)–P(3)–Os(3)	114.8(4)	C(311)–P(3)–Os(3)	118.4(3)
Os–C–O*	176.8		

* Average value.

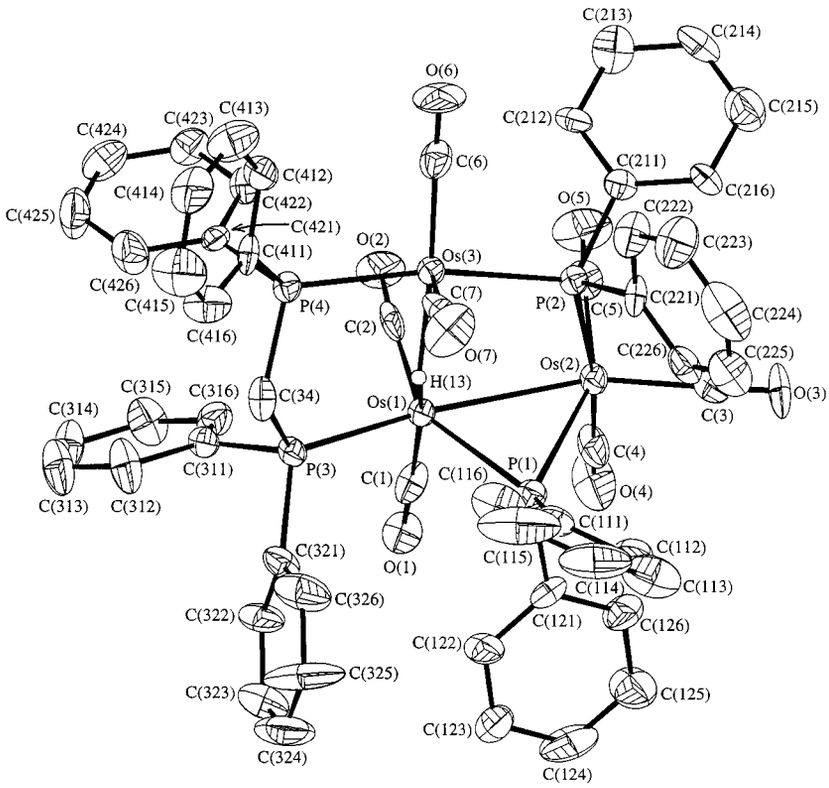

Fig. 2 Solid-state structure of $[Os_3H(\mu\text{-}H)(CO)_7(\mu\text{-dppm})(\mu\text{-}PPh_2)_2]\cdot H_2O$ **4**. The hydrogen atoms (except the bridging hydride) are omitted for clarity. Other details as in Fig. 1

Os–Os distance [Os(1)–Os(2) 2.8805(7) Å] is slightly longer than the unbridged Os(2)–Os(3) bond [2.8604(8) Å] but is similar to the other unbridged Os(1)–Os(3) bond [2.8790(8) Å] and comparable with the Os–Os distance in $[Os_3(CO)_{12}]$ [2.877(3) Å].[24] This observation is in contrast to $[Ru_3(CO)_{10}(\mu\text{-dppm})]$,[25] $[Ru_3(CO)_8(\mu\text{-dppm})_2]$,[26] $[Os_3(CO)_8(\mu\text{-dppm})_2]$,[4] $[Os_3(\mu\text{-}H)(CO)_8(\mu\text{-OH})(\mu\text{-dppm})]$[5] and $[Os_3(CO)_8(\mu\text{-dppm})(PPh_3)_2]$ in which the bridged metal–metal bonds are significantly shorter than the unbridged ones but is similar to that of $[Os_3(CO)_8(\mu\text{-dppm})\{P(OMe)_3\}_2]$[11] in which the bridged metal–metal bond is longer than the unbridged ones. The Os–C bond lengths [1.85(2)–1.93(2), average 1.89(2) Å] are comparable with those found in $[Os_3(CO)_{12}]$[24] and $[Os_3(CO)_9(\mu\text{-dppm})(\text{dppm-}P)]$.[13] The Os–C–O angles lie in the range 174.6(11)–177(2)° showing only small deviations from linearity. The Os–P bond lengths involving the bridging dppm ligand [Os(1)–P(1) 2.338(3) and Os(2)–P(2) 2.317(3) Å] are comparable with the corresponding values Os(2)–P(2) 2.336(6) and Os(1)–P(1) 2.315(6) Å found in $[Os_3(CO)_9(\mu\text{-dppm})(\text{dppm-}P)]$.[13] The Os(3)–P(3) distance involving the terminally bonded $PHPh_2$ has also a very similar value 2.325(3) Å. The Os–P–C and C–P–C angles are respectively greater [111.9(4)–119.5(4)°] and smaller [98.0(5)–107.7(6)°] than the ideal tetrahedral angle 109.47°, which may be explained by interligand steric interactions.

The ^{1}H NMR spectroscopic studies on compound **4** provided little information on the structure of the cluster because of the presence of more than one isomer in solution (see below). Therefore it was of interest to perform a single-crystal X-ray diffraction study of **4**. The sample used was crystallized from hexane–CH_2Cl_2 and found to contain two half-occupied water molecules (without any significant contacts with the complex) indicating slight contamination of the solvents or one of the starting materials. Discussion of the ^{1}H NMR spectroscopic data for **4** is deferred until X-ray diffraction results have been presented. The molecular structure is displayed in Fig. 2 and selected bond distances and angles are listed in Table 2.

Compound **4** consists of an osmium triangle with two diphenylphosphido moieties bridging across one bonding and one non-bonding Os–Os edge. The third Os–Os edge (bonding) is simultaneously bridged by the hydride and the dppm ligand. Both the μ-PPh_2 moieties act as three-electron donors and as usual the bridging dppm ligand donates four electrons to the cluster which results in a total of 50 valence electrons, and the observation of only two formal Os–Os bonds present in the trinuclear framework is consistent with the electron count. Of the two phosphido-bridged edges, Os(2)–Os(3) and Os(1)–Os(2), the former shows a non-bonding distance of 3.9952(9) Å whilst the latter bears the typical bonding Os–Os distance of 2.8733(9) Å, similar to the Os–Os distance in $[Os_3(CO)_{12}]$ [2.877(3) Å].[24] Thus the Os(1)–Os(2) bond length is unaffected by the introduction of the bridging phosphido group. The bridging hydride was located (but not refined) along the Os(1)–Os(3) edge, with distances of 1.66 and 1.84 Å from Os(1) and Os(3) respectively, and an Os(1)–H(13)–Os(3) angle 128°. The terminal hydride was not located directly but the distribution of the carbonyl groups indicated that it is bonded with Os(3) in a direction opposite to the Os(3)–C(7) bond. This arrangement of the hydride ligands is consistent with the NMR data (see below). As expected, the bond length between the two Os atoms bridged by the dppm ligand and the hydride ligand [Os(1)–Os(3) 3.1486(8) Å] is considerably longer than the other Os–Os bond [Os(1)–Os(2) 2.8733(9) Å]. This is consistent with the fact that a bridging hydride on a metal cluster causes significant lengthening of the bridged metal–metal edge if the presence of another bridging ligand along the same edge does not have any bond-shortening effect.[18,27] This conclusion is further supported by the large Os(1)–Os(3)–C(7) angle of 113.4(4)° to accommodate the bridging hydride. It may be noted that the Os(2)–P(1) distance of 2.392(4) Å is 0.029 Å longer than the Os(1)–P(1) distance of 2.363(3) and the Os(2)–P(2) distance of 2.469(3) Å is 0.066 Å longer than the Os(3)–P(2) distance of 2.403(4) Å. These differences in Os–P bond lengths appear to be real and indicate the asymmetric nature of the phosphido bridges. The Os(1)–P(1) and Os(2)–P(1) distances are comparable with values observed for related molecules where a phosphido group bridges a strong metal–metal bond.[18,19,28] The

Table 2 Selected bond lengths (Å) and angles (°) for $[Os_3H(\mu\text{-}H)(CO)_7(\mu\text{-dppm})(\mu\text{-}PPh_2)_2]\cdot H_2O$ **4**

Os(1)–Os(2)	2.8733(9)	Os(1)–Os(3)	3.1486(8)
Os(1)–P(3)	2.327(4)	Os(1)–P(1)	2.363(3)
Os(2)–P(1)	2.392(4)	Os(2)–P(2)	2.469(3)
Os(3)–P(4)	2.364(4)	Os(3)–P(2)	2.403(4)
Os(1)–H(13)	1.66	Os(3)–H(13)	1.84
Os–C(CO)*	1.93	C–O*	1.12
C(1)–Os(1)–C(2)	88.5(6)	C(1)–Os(1)–P(3)	90.5(5)
C(2)–Os(1)–P(3)	100.9(4)	C(1)–Os(1)–P(1)	90.0(4)
C(2)–Os(1)–P(1)	144.5(4)	P(3)–Os(1)–P(1)	114.53(13)
C(1)–Os(1)–Os(2)	97.4(5)	C(2)–Os(1)–Os(2)	91.8(4)
P(3)–Os(1)–Os(2)	165.21(9)	P(1)–Os(1)–Os(2)	53.29(9)
C(1)–Os(1)–Os(3)	171.0(5)	C(2)–Os(1)–Os(3)	82.5(4)
P(3)–Os(1)–Os(3)	91.18(9)	P(1)–Os(1)–Os(3)	97.39(9)
Os(2)–Os(1)–Os(3)	82.99(2)	C(3)–Os(2)–C(4)	94.2(6)
C(3)–Os(2)–C(5)	101.7(6)	C(4)–Os(2)–C(5)	88.3(6)
C(3)–Os(2)–P(1)	108.0(4)	C(4)–Os(2)–P(1)	86.7(5)
C(5)–Os(2)–P(1)	150.2(4)	C(3)–Os(2)–P(2)	94.2(5)
C(4)–Os(2)–P(2)	170.0(5)	C(5)–Os(2)–P(2)	84.7(4)
P(1)–Os(2)–P(2)	95.80(12)	C(3)–Os(2)–Os(1)	160.1(4)
C(4)–Os(2)–Os(1)	88.3(4)	C(5)–Os(2)–Os(1)	98.1(4)
P(1)–Os(2)–Os(1)	52.37(8)	P(2)–Os(2)–Os(1)	85.64(8)
C(7)–Os(3)–C(6)	91.0(6)	C(7)–Os(3)–P(4)	87.9(5)
C(6)–Os(3)–P(4)	97.1(4)	C(7)–Os(3)–P(2)	97.0(5)
C(6)–Os(3)–P(2)	95.3(4)	P(4)–Os(3)–P(2)	166.56(12)
C(7)–Os(3)–Os(1)	113.4(4)	C(6)–Os(3)–Os(1)	155.6(5)
P(4)–Os(3)–Os(1)	85.75(8)	P(2)–Os(3)–Os(1)	80.82(8)
C(121)–P(1)–C(111)	101.1(5)	C(121)–P(1)–Os(1)	116.2(3)
C(111)–P(1)–Os(1)	128.3(4)	C(121)–P(1)–Os(2)	114.1(4)
C(111)–P(1)–Os(2)	122.3(4)	Os(1)–P(1)–Os(2)	74.34(10)
C(221)–P(2)–C(211)	97.6(4)	C(221)–P(2)–Os(3)	109.7(3)
C(211)–P(2)–Os(3)	114.8(3)	C(221)–P(2)–Os(2)	117.5(4)
C(211)–P(2)–Os(2)	106.7(3)	Os(3)–P(2)–Os(2)	110.18(13)
C(34)–P(3)–C(311)	105.4(5)	C(34)–P(3)–C(321)	102.3(6)
C(311)–P(3)–C(321)	99.0(5)	C(34)–P(3)–Os(1)	113.1(5)
C(311)–P(3)–Os(1)	119.0(3)	C(321)–P(3)–Os(1)	115.8(4)
C(411)–P(4)–C(421)	103.5(4)	C(411)–P(4)–C(34)	103.8(5)
C(421)–P(4)–C(34)	105.2(5)	C(411)–P(4)–Os(3)	112.9(3)
C(421)–P(4)–Os(3)	121.1(3)	C(34)–P(4)–Os(3)	108.0(4)
Os(1)–H(13)–Os(3)	128	Os–C–O*	175.5

* Average value.

Os–P distances involving the bridging dppm ligand 2.327(4) and 2.364(4) Å are also somewhat asymmetric and generally shorter than those involving the phosphide ligands; these values are also slightly shorter than the corresponding values in compound **3**. As expected, the Os(1)–P(1)–Os(2) angle [74.34(10)°] is much narrower than the Os(2)–P(2)–Os(3) angle [110.18(13)°] due to metal–metal bonding along the Os(1)–Os(2) edge. The Os–P(1)–C angles [114.1(4)–128.3(4)°] are generally wider than the Os–P(2)–C angles [106.7(3)–117.5(4)°]; similarly, the Os–P(4)–C angles [108.8(4)–121.1(3)°] are wider than those [113.1(5)–119.0(3)°] at P(3). These angular variations at chemically equivalent atoms may be explained in terms of steric interactions.

Having established the molecular structure of compound **4** it is possible to interpret the ^{1}H NMR spectrum of the cluster. This consists of a complex multiplet for the aromatic protons (40 H) centred at δ 7.34, three sets of quartets at δ 4.63, 3.67 and 3.49 attributable to the methylene protons of the dppm ligand and four sets of multiplets at δ −9.15, −15.13, −16.12 and −16.99 for the hydride ligands. The two methylene protons appear as three sets of quartets in a ratio of 5:3:1 and the bridging hydride appears as three sets of multiplets of approximate ratio 5:3:1 while the terminal hydride resonances appears as overlapping multiplets of integral area equal to the sum of those of the three bridging hydride resonances. These data clearly indicate the presence of three possible terminal hydride location isomers of **4** in solution.

The formation of compound **4** can be envisaged as occurring *via* the bis(diphenylphosphine)-substituted cluster $[Os_3(CO)_8(\mu\text{-dppm})(PHPh_2)_2]$ **6** followed by P–H activation and cleavage of a metal–metal bond (Scheme 3). We have demonstrated this by synthesizing cluster **6**. Treatment of a toluene solution of the unsaturated cyclometallated cluster $[Os_3(\mu\text{-}H)(CO)_8\{Ph_2PCH_2P(Ph)C_6H_4\}]$ **2** with an excess of $PHPh_2$ at room temperature affords the adducts $[Os_3(\mu\text{-}H)(CO)_8\{Ph_2PCH_2P(Ph)C_6H_4\}(PHPh_2)]$ **5** and $[Os_3(CO)_8(\mu\text{-dppm})(PHPh_2)_2]$ **6** in 16 and 62% yields respectively (Scheme 3).

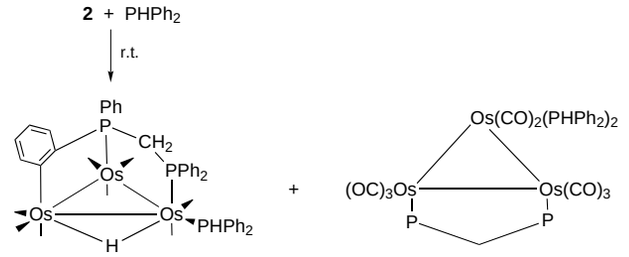

5 6

Scheme 3

The elemental analysis, IR spectrum and ^{1}H and ^{31}P-{^{1}H} NMR spectroscopic data for cluster **5** are fully consistent with the proposed structure. The IR spectrum in the carbonyl stretching region is closely similar to that reported for the corresponding $P(OMe)_3$ analogue $[Os_3(\mu\text{-}H)(CO)_8\{Ph_2PCH_2P(Ph)C_6H_4\}\{P(OMe)_3\}]$ suggesting that **5** adopts a very similar structure to that established by a single-crystal X-ray diffraction study for the $P(OMe)_3$ compound.[11] The ^{1}H NMR spectrum of **5** in the hydride region contains a doublet of triplets at δ −16.65, in accord with the proposed structure. The ^{31}P-{^{1}H} NMR spectrum consists of three doublet of doublets at δ −20.9 (dd, J = 6.4, 27.5), −16.9 (dd, J = 75.1, 27.5) and −12.3 (dd, J = 75.1, 6.4 Hz). The ^{1}H and ^{31}P-{^{1}H} NMR spectroscopic data and the magnitudes of the phosphorus–hydrogen and –phosphorus couplings are very similar to those previously observed[11] for the $P(OMe)_3$ analogue which again suggests a close similarity between the structures.

Compound **6** has been characterized by elemental analysis, infrared, ^{1}H and ^{31}P-{^{1}H} NMR spectroscopic data and as well as single-crystal X-ray diffraction analysis. The infrared spectrum in the carbonyl stretching region closely resembles that reported[11] for the $P(OMe)_3$ analogue $[Os_3(CO)_8(\mu\text{-dppm})\{P(OMe)_3\}_2]$ suggests that they have very similar structures. In the ^{1}H NMR spectrum of **6** the $PHPh_2$ protons appear as a doublet at δ 7.23 (J = 375.7 Hz) indicating that the $PHPh_2$ ligands are equivalent while the methylene protons of the dppm ligand appear as a triplet at δ 4.85 (J = 10.3 Hz) indicating that the ^{31}P nuclei of the dppm ligand are also equivalent. The ^{31}P-{^{1}H} NMR spectrum shows two singlets at δ −27.7 and −25.3 while the proton-coupled ^{31}P spectrum contains a doublet at δ −25.3 (J_{PH} = 378.2 Hz) and a singlet at δ −27.7 indicating that the former signal is due to the $PHPh_2$ ligand while the latter is due to the bridging dppm ligand.

The solid-state structure of compound **6** was elucidated by a single-crystal X-ray diffraction study. The molecular structure is shown in Fig. 3 and selected bond distances and angles are given in Table 3. The molecule consists of a triangular cluster of three osmium atoms with all the four phosphorus atoms in the equatorial plane. The structure is similar to that of $[Os_3(CO)_8(\mu\text{-dppm})\{P(OMe)_3\}_2]$ both in terms of osmium–phosphorus framework and ligand arrangement, with the osmium–osmium distances short enough to indicate the existence of three metal–metal bonds. The bridged Os–Os distance [Os(1)–Os(2) 2.9021(9) Å] is slightly longer than the non-bridged Os–Os distances [Os(1)–Os(3) 2.8858(9) and Os(2)–Os(3) 2.8920(10) Å]. Both the $PHPh_2$ ligands are coordinated at equatorial sites on Os(3). The Os–P bonds are marginally longer for the dppm [Os(1)–P(1) 2.313(4) and Os(2)–P(2) 2.328(4) Å] than for the phosphines [Os(3)–P(3)

Table 3 Selected bond lengths (Å) and angles (°) for $[Os_3(CO)_8(\mu\text{-dppm})(PHPh_2)_2]$ **6**

Os(1)–Os(3)	2.8858(9)	Os(1)–Os(2)	2.9021(9)
Os(2)–Os(3)	2.8920(10)	Os(1)–P(1)	2.313(4)
Os(2)–P(2)	2.328(4)	Os(3)–P(4)	2.281(4)
Os(3)–P(3)	2.295(4)	Os–C(CO)*	1.93
C–O*	1.15		
C(2)–Os(1)–C(3)	92.4(6)	C(2)–Os(1)–C(1)	90.1(6)
C(3)–Os(1)–C(1)	172.7(6)	C(2)–Os(1)–P(1)	100.0(4)
C(3)–Os(1)–P(1)	95.0(5)	C(1)–Os(1)–P(1)	91.4(4)
C(2)–Os(1)–Os(3)	107.7(4)	C(3)–Os(1)–Os(3)	89.9(4)
C(1)–Os(1)–Os(3)	82.8(4)	P(1)–Os(1)–Os(3)	151.59(9)
C(2)–Os(1)–Os(2)	165.5(4)	C(3)–Os(1)–Os(2)	80.5(4)
C(1)–Os(1)–Os(2)	95.5(4)	P(1)–Os(1)–Os(2)	93.25(9)
Os(3)–Os(1)–Os(2)	59.95(2)	C(5)–Os(2)–C(4)	89.3(6)
C(5)–Os(2)–C(6)	91.8(7)	C(4)–Os(2)–C(6)	166.8(7)
C(5)–Os(2)–P(2)	101.1(5)	C(4)–Os(2)–P(2)	99.4(5)
C(6)–Os(2)–P(2)	93.3(5)	C(5)–Os(2)–Os(3)	110.7(4)
C(4)–Os(2)–Os(3)	78.3(5)	C(6)–Os(2)–Os(3)	89.0(5)
P(2)–Os(2)–Os(3)	147.99(10)	C(5)–Os(2)–Os(1)	167.2(5)
C(4)–Os(2)–Os(1)	96.5(5)	C(6)–Os(2)–Os(1)	80.0(5)
P(2)–Os(2)–Os(1)	89.22(10)	Os(3)–Os(2)–Os(1)	59.74(2)
C(8)–Os(3)–C(7)	177.0(6)	C(8)–Os(3)–P(4)	94.2(4)
C(7)–Os(3)–P(4)	88.8(4)	C(8)–Os(3)–P(3)	89.9(4)
C(7)–Os(3)–P(3)	89.6(4)	P(4)–Os(3)–P(3)	101.43(14)
C(8)–Os(3)–Os(1)	92.1(4)	C(7)–Os(3)–Os(1)	87.7(4)
P(4)–Os(3)–Os(1)	91.02(10)	P(3)–Os(3)–Os(1)	167.22(10)
C(8)–Os(3)–Os(2)	83.5(4)	C(7)–Os(3)–Os(2)	93.8(4)
P(4)–Os(3)–Os(2)	151.01(10)	P(3)–Os(3)–Os(2)	107.45(10)
Os(1)–Os(3)–Os(2)	60.30(2)	C(12)–P(1)–C(121)	104.9(6)
C(12)–P(1)–C(111)	102.2(6)	C(121)–P(1)–C(111)	100.5(5)
C(12)–P(1)–Os(1)	114.6(5)	C(121)–P(1)–Os(1)	118.0(3)
C(111)–P(1)–Os(1)	114.5(4)	C(211)–P(2)–C(221)	99.8(4)
C(211)–P(2)–C(12)	106.4(6)	C(221)–P(2)–C(12)	98.2(5)
C(211)–P(2)–Os(2)	120.1(3)	C(221)–P(2)–Os(2)	118.4(3)
C(12)–P(2)–Os(2)	111.1(5)	C(311)–P(3)–C(321)	102.4(5)
C(311)–P(3)–Os(3)	120.8(3)	C(321)–P(3)–Os(3)	118.3(4)
C(411)–P(4)–C(421)	103.2(4)	C(411)–P(4)–Os(3)	120.3(4)
C(421)–P(4)–Os(3)	119.2(3)	Os–C–O*	173.4

* Average value.

2.295(4) Å and Os(3)–P(4) 2.281(4) Å], and these are comparable with the corresponding values in **3**. The Os–P–C and C–P–C angles are also close to the respective values in **3**.

As expected thermolysis of compound **6** in refluxing toluene leads to the formation of **4** (29% yield) as the major product in addition to two isomeric novel compounds $[Os_3(\mu\text{-}H)_2(CO)_6(\mu\text{-dppm})(\mu\text{-}PPh_2)_2]$ **7** and $[Os_3(\mu\text{-}H)_2(CO)_6(\mu\text{-dppm})(\mu\text{-}PPh_2)_2]$ **8** as the minor products (Scheme 4) in 10 and 6% yields respectively. Compound **7** has been characterized by infrared, ^1H and $^{31}P\text{-}\{^1H\}$ NMR spectroscopic data, elemental analysis as well as a crystal structure determination. The molecular structure is depicted in Fig. 4 and selected bond distances and angles are listed in Table 4. The molecule consists of a triangular core of osmium atoms with three distinctly different osmium–osmium bond lengths: Os(1)–Os(2) 3.0094(13), Os(2)–Os(3) 2.9234(13), and Os(1)–Os(3) 2.8843(12) Å and six terminal carbonyl ligands, two on each metal atom. Each of the Os(1)–Os(3) and Os(2)–Os(3) edges is bridged by a PPh_2 and a hydride ligand while the Os(1)–Os(2) edge is bridged by the dppm ligand. The terminal $PHPh_2$ ligands in **6** have been transformed into bridging PPh_2 group in **7** by oxidative addition. The two phosphido groups lie respectively above and below the triosmium plane with P(4) occupying an axial site on Os(2) while P(3) is axial on Os(1). The Os(1)–Os(3) bond length of 2.8843(12) Å compares well with that in the closely related PPh_2- and hydride-bridged cluster $[Os_3(\mu\text{-}H)_2(CO)_8(\mu\text{-}PPh_2)_2]$ [2.8896(4) Å (average)][19] while the Os(2)–Os(3) edge at 2.9234(13) Å is significantly longer. The dppm-bridged Os(2)–Os(1) distance of 3.0094(13) Å is significantly longer than the corresponding distances in **3** [2.8805(7) Å] and **6** [2.9021(9) Å], but shorter than that in **4** [3.1486(8) Å]. The Os(3)–P(4) and Os(3)–P(3) bond lengths

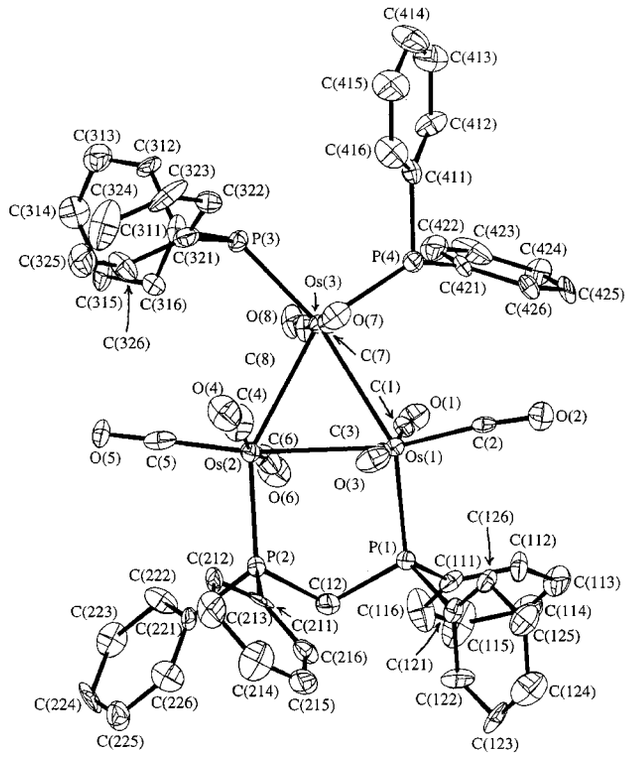

Fig. 3 Solid-state structure of $[Os_3(CO)_8(\mu\text{-dppm})(PHPh_2)_2]$ **6** showing the atom labelling scheme. Thermal ellipsoids are drawn at 50% probability level. The hydrogen atoms are omitted for clarity

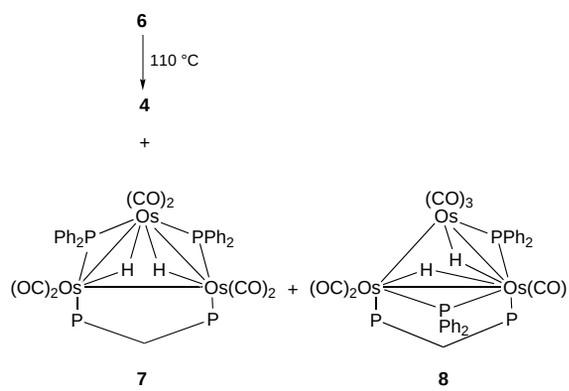

Scheme 4

[2.328(4) and 2.353(4) Å respectively] are significantly shorter than the Os(2)–P(4) and Os(1)–P(3) distances [2.373(5) and 2.426(5) Å respectively]. These Os–P distances are close to the values found in **4** and other related clusters where a phosphido group bridges a metal–metal bond.[18,19,22,28] The two Os–P–Os angles 74.24(13) and 76.90(13)° are nearly the same and close to the value at the phosphido phosphorus bridging the metal–metal bonded edge in **4**. Other geometry parameters for the diphenylphosphide and dppm ligands are as expected for this type of compounds. The average values for the Os–C (CO) and C–O (CO) distances and Os–C–O angles in **7** are 1.87, 1.16 Å and 175.8° respectively. These are comparable with the corresponding average values 1.89, 1.18 Å and 176.8° in **3**, 1.93, 1.12 Å, 176.2° in **4**, and 1.93, 1.15 Å and 173.4° in **6**.

The $^{31}P\text{-}\{^1H\}$ NMR spectrum of compound **7** contains four doublet of doublet of doublets at δ 67.6 (J = 161.2, 85.6, 7.7), 52.8 (J = 85.6, 26.8, 7.3), −14.9 (J = 72.3, 26.8, 7.3) and −20.9 (J = 161.2, 72.3, 7.3 Hz) indicating non-equivalence of all the four ^{31}P nuclei. In the ^1H NMR spectrum the hydrides appear as a doublet of doublets at δ −16.32 (J_{PH} = 22.8, 9.8 Hz) and a multiplet at δ −17.21 in relative intensity of 1:1. One of the hydrides shows additional couplings to the methylene protons

Table 4 Selected bond lengths (Å) and angles (°) for $[Os_3(\mu\text{-}H)_2(CO)_6(\mu\text{-}dppm)(\mu\text{-}PPh_2)_2]\cdot CH_2Cl_2$ **7**

Os(1)–Os(3)	2.8843(12)	Os(1)–Os(2)	3.0094(13)
Os(2)–Os(3)	2.9234(13)	Os(1)–P(1)	2.327(5)
Os(1)–P(3)	2.426(5)	Os(2)–P(2)	2.351(5)
Os(2)–P(4)	2.373(5)	Os(3)–P(4)	2.328(4)
Os(3)–P(3)	2.353(4)	Os(1)–H(13)	1.7
Os(3)–H(13)	1.98	Os(2)–H(23)	1.73
Os(3)–H(23)	1.68	Os–C(CO)*	1.87
C–O*	1.16		
C(1)–Os(1)–C(2)	90.3(7)	C(1)–Os(1)–P(1)	95.7(5)
C(2)–Os(1)–P(1)	102.7(5)	C(1)–Os(1)–P(3)	92.9(5)
C(2)–Os(1)–P(3)	158.4(5)	P(1)–Os(1)–P(3)	98.2(2)
C(1)–Os(1)–Os(3)	119.0(5)	C(2)–Os(1)–Os(3)	108.6(4)
P(1)–Os(1)–Os(3)	132.01(10)	P(3)–Os(1)–Os(3)	51.73(9)
C(1)–Os(1)–Os(2)	172.4(5)	C(2)–Os(1)–Os(2)	83.6(4)
P(1)–Os(1)–Os(2)	89.92(10)	P(3)–Os(1)–Os(2)	91.22(9)
Os(3)–Os(1)–Os(2)	59.43(3)	C(4)–Os(2)–C(3)	93.2(7)
C(4)–Os(2)–P(2)	89.8(5)	C(3)–Os(2)–P(2)	92.3(6)
C(4)–Os(2)–P(4)	93.0(5)	C(3)–Os(2)–P(4)	98.9(7)
P(2)–Os(2)–P(4)	168.3(2)	C(4)–Os(2)–Os(3)	118.9(5)
C(3)–Os(2)–Os(3)	133.7(6)	P(2)–Os(2)–Os(3)	118.16(11)
P(4)–Os(2)–Os(3)	50.87(11)	C(4)–Os(2)–Os(1)	175.8(5)
C(3)–Os(2)–Os(1)	90.9(4)	P(2)–Os(2)–Os(1)	89.44(10)
P(4)–Os(2)–Os(1)	86.99(10)	Os(3)–Os(2)–Os(1)	58.16(3)
C(5)–Os(3)–C(6)	86.3(7)	C(5)–Os(3)–P(4)	105.3(5)
C(6)–Os(3)–P(4)	100.4(5)	C(5)–Os(3)–P(3)	99.0(4)
C(6)–Os(3)–P(3)	109.6(5)	P(4)–Os(3)–P(3)	142.4(2)
C(5)–Os(3)–Os(1)	108.0(4)	C(6)–Os(3)–Os(1)	159.0(5)
P(4)–Os(3)–Os(1)	90.84(11)	P(3)–Os(3)–Os(1)	54.04(11)
C(5)–Os(3)–Os(2)	152.6(5)	C(6)–Os(3)–Os(2)	111.2(5)
P(4)–Os(3)–Os(2)	52.23(12)	P(3)–Os(3)–Os(2)	94.88(12)
Os(1)–Os(3)–Os(2)	62.42(3)	C(12)–P(1)–Os(1)	113.0(5)
C(111)–P(1)–Os(1)	116.1(4)	C(121)–P(1)–Os(1)	121.0(4)
C(221)–P(2)–Os(2)	113.4(5)	C(12)–P(2)–Os(2)	116.8(5)
C(211)–P(2)–Os(2)	117.8(4)	C(311)–P(3)–Os(3)	112.7(4)
C(321)–P(3)–Os(3)	123.1(3)	C(311)–P(3)–Os(1)	117.6(4)
C(321)–P(3)–Os(1)	128.0(4)	Os(3)–P(3)–Os(1)	74.24(13)
C(411)–P(4)–Os(3)	119.4(4)	C(421)–P(4)–Os(3)	116.6(4)
C(411)–P(4)–Os(2)	119.6(4)	C(421)–P(4)–Os(2)	117.5(4)
Os(3)–P(4)–Os(2)	76.90(13)	Os(1)–H(13)–Os(3)	103
Os(2)–H(23)–Os(3)	118	Os–C–O*	176.2

* Average value.

of the dppm ligand and appears as a multiplet at δ −17.21 which has been confirmed by recording ^{31}P-decoupled ^{1}H NMR spectra. Similar couplings of the methylene protons of a dppm ligand with bridging hydride has been reported.[10] Thus the ^{1}H and ^{31}P-{^{1}H} NMR spectroscopic data are fully consistent with the structure.

We were unable to obtain X-ray-quality crystals of compound **8**, therefore the characterization is based on infrared, ^{1}H NMR, elemental analysis and the crystal structure of **7**. The ^{1}H NMR spectrum in the hydride region contains two equally intense multiplets at δ −15.55 and −18.93. In the ^{31}P-{^{1}H} NMR spectrum the inequivalence of all the ^{31}P nuclei is clearly shown by resonances at δ 65.8 (ddd, J = 154.5, 55.8, 32.3), 52.5 (ddd, J = 55.8, 48.5, 7.6), −16.9 (ddd, J = 154.5, 72.5, 7.6) and −22.1 (ddd, J = 72.5, 45.8, 32.3 Hz). We believe that **8** is an isomer of **7** in which one hydride and one phosphide ligand bridge the same edge as the dppm ligand while the other hydride and phosphide ligand bridge one of the remaining Os–Os edges. This result clearly indicates that in the reaction of **1** with $PHPh_2$ the dihydrido cluster **4** is formed *via* the formation of **6** followed by subsequent decarbonylation, P–H activation and cleavage of an osmium–osmium bond.

Thermolysis of compound **3** in toluene at 110 °C leads to the formation of $[Os_3(\mu\text{-}H)(CO)_8(\mu\text{-}dppm)(\mu\text{-}PPh_2)]$ **9** in 55% yield. Compound **9** results from the activation of a P–H bond and has been characterized on the basis of IR, ^{1}H and ^{31}P-{^{1}H} NMR spectroscopic data and elemental analysis. The ^{1} H NMR spectrum, in the hydride region, shows two sets of doublet of doublets at δ −13.30 (J_{PH} = 9.7, 17.1) and −13.45 (J_{PH} = 9.6, 17.0 Hz) in approximate 1 : 1 ratio. The metal hydride signal shows coupling to the two non-equivalent phosphorus atoms. The ^{31}P-{^{1}H} NMR spectrum contains signals for two isomers, three doublet of doublets for each. Thus the ^{1}H and ^{31}P-{^{1}H} NMR data clearly indicate that compound **9** exists as two isomeric forms in solution. There are several isomers possible. However, the formation of two containing different relative positions of the phosphide and the hydride ligand can easily be envisaged. Based on ^{1}H and ^{31}P-{^{1}H} NMR spectroscopic data, they are proposed to have the structures depicted in Scheme 5.

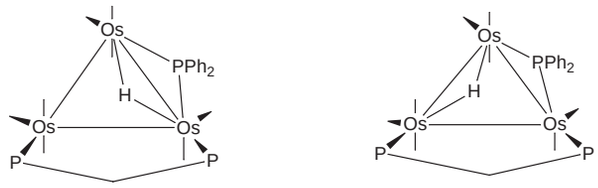

9a **9b**

Scheme 5

Assuming that in one of the structures the hydride is bridging the same Os–Os edge as the phosphido moiety gives rise to isomer **9a**. The migration of the hydride from **9a** to the unsupported edge leads to isomer **9b**. Another possible structure with the hydride bridging the same edge as the dppm can be ruled out since one wold expect a hydride doublet or doublet of doublets for such a structure. However, due to the lack of good-quality crystals, the structure of **9** could not be confirmed by diffraction methods.

Thermolysis of compound **4** at 110 °C for 16 h also leads to the formation of the isomeric compounds **7** and **8** in 28 and 16% yields respectively. The formation of **7** and **8** from **4** involves removal of CO followed by reformation of a metal–metal bond. These complexes are also accessible *via* the decarbonylation of **6**.

Experimental

The general experimental techniques were as described previously.[29] Proton and ^{31}P NMR spectra were obtained on a Bruker AC-200 spectrometer with tetramethylsilane (internal) and 85% H_3PO_4 (external) as standards. Elemental analyses were carried out at the Microanalytical Laboratory, Institut für Anorganische und Analytische Chemie, Universität Freiburg. The starting clusters **1** and **2** were prepared according to the published procedures.[3,7]

Reactions with $PHPh_2$

Compound 1. To a toluene solution (30 cm^3) of compound **1** (0.105 g, 0.085 mmol) was added $PHPh_2$ (0.047 g, 0.085 mmol) and the reaction mixture refluxed for 5 h. The solvent and excess of $PHPh_2$ were removed *in vacuo* and the residue was subjected to TLC on silica gel. Elution with hexane–CH_2Cl_2 (3 : 1, v/v) gave three bands. The faster moving band gave unchanged **1** (0.005 g). The second band afforded $[Os_3(CO)_9(\mu\text{-}dppm)(PHPh_2)]$ **3** (0.083 g, 70%) as red crystals after recrystallization from hexane–CH_2Cl_2 at −20 °C (Found: C, 39.61; H, 2.29. Calc. for $C_{46}H_{33}O_9Os_3P_3$: C, 39.66; H, 2.39%). IR [ν(CO), CH_2Cl_2]: 2062m, 1997s, 1979vs, 1956m and 1932m cm^{-1}. ^{1}H NMR ($CDCl_3$): δ 6.35 (m, 40 H), 6.29 (d, 1H, J_{PH} = 383.4) and 3.82 (t, 2 H, J_{PH} = 10.4 Hz). ^{31}P-{^{1}H} NMR ($CDCl_3$): δ 10.9 (d, J = 54.7), 12.5 (d, J = 54.7 Hz) and 38.8 (s). The third band yielded $[Os_3H(\mu\text{-}H)(CO)_7(\mu\text{-}dppm)(\mu\text{-}PPh_2)_2]\cdot H_2O$ **4** (0.020 g, 15%) as pale yellow crystals after recrystallization from hexane–CH_2Cl_2 at −20 °C (Found: C, 43.45; H, 2.98. Calc. for $C_{56}H_{46}O_8Os_3P_4$: C, 43.63; H, 3.01%). IR [ν(CO), CH_2Cl_2]: 2126s, 2051vs, 2015m, 1992vs, 1975s, 1941s, 1922m and 1918m cm^{-1}. ^{1}H NMR ($CDCl_3$): mixture of three isomers, δ 7.34 (m,

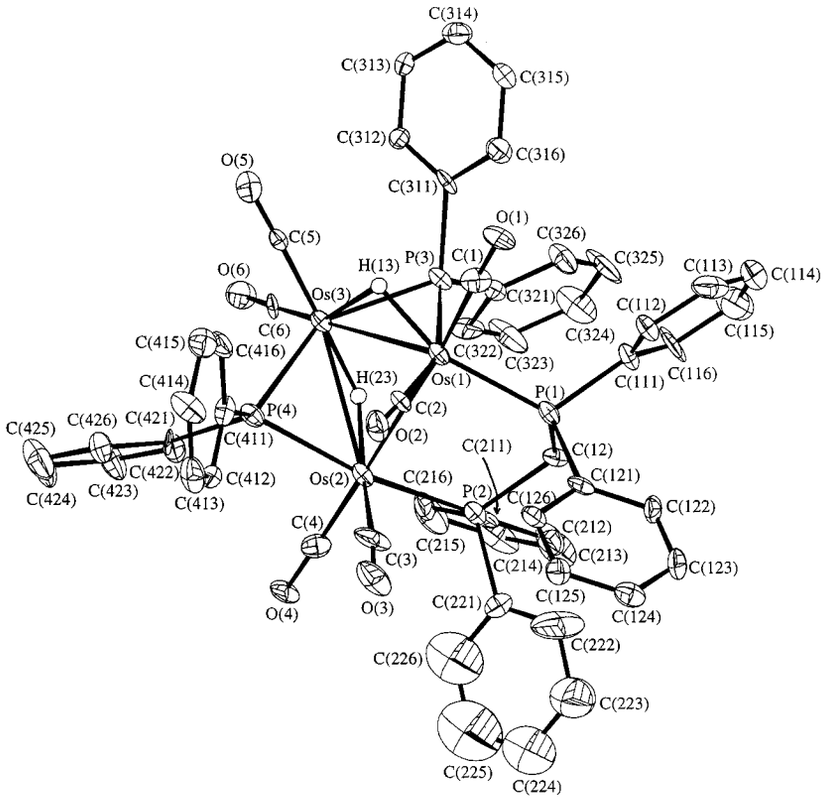

Fig. 4 Solid-state structure of $[Os_3(\mu\text{-}H)_2(CO)_6(\mu\text{-dppm})(PPh_2)_2]\cdot CH_2Cl_2$ **7**. The hydrogen atoms (except the bridging hydrides) are omitted for clarity. Other details as in Fig. 3

40 H), 4.63 (q, 2 H), 3.67 (q, 2 H), 3.49 (q, 2 H) −9.15 (overlapping multiplets for the three isomers), −15.13 (m, 1 H), −16.12 (m, 1 H) and −16.99 (m, 1 H). The phenyl proton resonances of the isomers are overlapped.

$[Os_3(\mu\text{-}H)(CO)_8\{Ph_2PCH_2P(Ph)C_6H_4\}]$ 2. An excess of $PHPh_2$ (0.069 g, 0.371 mmol) was added to a toluene solution (15 cm^3) of compound **2** (0.174 g, 0.125 mmol) and the reaction mixture stirred at room temperature for 30 min during which time it changed from green to yellow. The solvent was removed under reduced pressure and the residue subjected to TLC on silica gel. Elution with hexane–CH_2Cl_2 (10:3, v/v) resolved two bands. The first band afforded $[Os_3(\mu\text{-}H)(CO)_8\{Ph_2PCH_2\text{-}P(Ph)C_6H_4\}(PHPh_2)]$ **5** (0.030 g, 16%) as yellow crystals after recrystallization from hexane–CH_2Cl_2 at −20 °C (Found: C, 35.65; H, 2.38. Calc. for $C_{45}H_{33}O_8Os_3P_3$: C, 35.48; H, 2.19%). IR [ν(CO), CH_2Cl_2]: 2056vs, 2019s, 1997s, 1977s, 1963w, 1942w and 1923w cm^{-1}. ^1H NMR ($CDCl_3$): δ 7.92–5.88 (m, 30 H), 3.63 (dt, 2 H, J = 9.6, 3.1) and −16.65 (dt, 1 H, J = 10.3, 1.3 Hz). The phenyl protons of the dppm ligand and the $PHPh_2$ protons are overlapped. $^{31}P\text{-}\{^1H\}$ NMR ($CDCl_3$): δ −20.9 (dd, J = 6.4, 27.5), −16.9 (dd, J = 75.1, 27.5) and −12.3 (dd, J = 75.1, 6.4 Hz). The second band yielded $[Os_3(CO)_8(\mu\text{-dppm})(PHPh_2)_2]$ **6** (0.120 g, 62%) as orange crystals after recrystallization from hexane–CH_2Cl_2 (Found: C, 44.31; H, 2.95. Calc. for $C_{57}H_{44}\text{-}O_8Os_3P_4$: C, 44.13; H, 2.86%). IR [ν(CO), CH_2Cl_2] 2043w, 1986s, 1963vs and 1920m cm^{-1}. ^1H NMR ($CDCl_3$): δ 7.39–7.24 (m, 40 H), 7.23 (d, 2 H, J = 375.7) and 4.85 (t, 2 H, J = 10.3 Hz). $^{31}P\text{-}\{^1H\}$ NMR ($CDCl_3$): δ −27.7 (s) and −25.3 (s). ^{31}P NMR ($CDCl_3$): δ −27.7 (s) and −25.3 (d, J_{PH} = 378.2 Hz).

Thermoylses

Compound 6. A toluene solution (20 cm^3) of compound **6** (0.070 g, 0.046 mmol) was heated to reflux for 3 h. The solvent was removed by rotary evaporation and the residue subjected to TLC on silica gel. Elution with hexane–CH_2Cl_2 (2:1, v/v) gave three bands. The faster moving band gave **4** (0.020 g, 29%). The second afforded $[Os_3(\mu\text{-}H)_2(CO)_6(\mu\text{-dppm})(\mu\text{-}PPh_2)_2]\cdot CH_2Cl_2$ **7** (0.007 g, 10%) as pale yellow crystals from hexane–CH_2Cl_2 (Found: C, 44.30; H, 3.15. Calc. for $C_{55}H_{44}O_6Os_3P_4$: C, 44.17; H, 2.97%). IR [ν(CO), CH_2Cl_2]: 2065s, 2025s, 1989vs, 1962m and 1923w cm^{-1}. ^1H NMR (CD_2Cl_2): δ 8.04–6.58 (m, 40 H), 2.67 (m, 2 H), −16.32 (dd, 1 H, J_{PH} = 22.8, 9.8 Hz) and −17.21 (m, 1 H). $^{31}P\text{-}\{^1H\}$ NMR: δ 67.6 (ddd, J = 161.2, 85.6, 7.7), 52.8 (ddd, J = 85.6, 26.8, 7.3), −14.9 (ddd, J = 72.3, 26.8, 7.3) and −20.9 (ddd, J = 161.2, 72.3, 7.3 Hz). The third band gave $[Os_3(\mu\text{-}H)_2(CO)_6(\mu\text{-dppm})(\mu\text{-}PPh_2)_2]$ **8** (0.004 g, 6%) as yellow crystals from hexane–CH_2Cl_2 (Found: C, 44.45; H, 3.32. Calc. for $C_{55}H_{44}O_6Os_3P_4$: C, 44.17; H, 2.97%). IR [ν(CO), CH_2Cl_2]: 2064s, 2023s, 1986vs, 1966w, 1960w and 1922w cm^{-1}. ^1H NMR ($CDCl_3$): δ 7.99–6.78 (m, 40 H), 4.29 (m, 2 H), −15.55 (m, 1 H) and −18.93 (m, 1 H), $^{31}P\text{-}\{^1H\}$ NMR ($CDCl_3$): δ 65.8 (ddd, J = 154.5, 55.8, 32.3), 52.5 (ddd, J = 55.8, 48.5, 7.6), −16.9 (ddd, J = 154.5, 72.5, 7.6) and −22.1 (ddd, J = 72.5, 45.8, 32.3 Hz).

Compound 3. The cluster **3** (0.065 g, 0.047 mmol) in toluene (30 cm^3) was heated under reflux for 8 h. The solvent was removed under reduced pressure and the residue subjected to TLC on silica gel. Elution with hexane–CH_2Cl_2 (2:1, v/v) gave one band which afforded $[Os_3(\mu\text{-}H)(CO)_8(\mu\text{-dppm})(\mu\text{-}PPh_2)]$ **9** (0.035 g, 55%) as yellow crystals after recrystallization from acetone–ethanol at −20 °C (Found: C, 39.85; H, 2.64. Calc. for $C_{45}H_{33}O_8Os_3P_3$: C, 39.59; H, 2.44%). IR [ν(CO), CH_2Cl_2]: 2046w, 2022vs, 1989s, 1950m, 1932m and 1918m cm^{-1}. ^1H NMR ($CDCl_3$): mixture of two isomers, δ 7.76–6.98 (m, 30 H), 3.79 (q, 2 H), −13.30 (dd, 1 H, J_{PH} = 17.1, 9.7) and −13.45 (dd, 1 H, J_{PH} = 17.0, 9.6 Hz). The peaks due to the methylene and phenyl protons for the isomers are overlapped. $^{31}P\text{-}\{^1H\}$ NMR ($CDCl_3$): δ 163.5 (dd, J = 174.3, 19.9), 163.5 (dd, J = 174.5, 19.8), −16.1 (dd, J = 44.9, 19.8), −16.4 (dd, J = 44.9, 19.8), −40.1 (dd, J = 174.3, 44.9) and −40.4 (dd, J = 44.9, 19.8 Hz).

Compound 4. A similar thermolysis of compound **4** (0.025 g, 0.016 mmol) in toluene (15 cm^3) for 16 h followed by similar

Table 5 Crystal data and details of data collection and structure refinement for $[Os_3(CO)_9(\mu\text{-dppm})(PHPh_2)]$ **3**, $[Os_3H(\mu\text{-H})(CO)_7(\mu\text{-dppm})(\mu\text{-PPh}_2)_2]\cdot H_2O$ **4**, $[Os_3(CO)_8(\mu\text{-dppm})(PHPh_2)_2]$ **6** and $[Os_3(\mu\text{-H})_2(CO)_6(\mu\text{-dppm})(PPh_2)_2]\cdot CH_2Cl_2$ **7**

	3	**4**	**6**	**7**
Empirical formula	$C_{46}H_{33}O_9Os_3P_3$	$C_{56}H_{44}O_7Os_3P_4\cdot H_2O$	$C_{57}H_{44}O_8Os_3P_4$	$C_{55}H_{44}O_6Os_3P_4\cdot CH_2Cl_2$
M	1393.23	1541.41	1551.40	1580.31
T/K	293(2)	293(2)	150(2)	150(2)
Crystal system	Monoclinic	Monoclinic	Orthorhombic	Triclinic
Space group	$P2_1/c$ (no. 14)	$P2_1/n$ (no. 14)	$Pna2_1$ (no. 33)	$P\bar{1}$ (no. 2)
a/Å	18.735(3)	12.339(2)	29.460(8)	12.040(4)
b/Å	13.930(3)	20.625(3)	18.247(4)	13.376(4)
c/Å	18.368(2)	23.859(3)	9.753(4)	18.688(7)
α/°				83.30(2)
β/°	109.78(2)	102.809(5)		73.45(3)
γ/°				87.48(2)
U/Å^3	4510.8(13)	5921(2)	5243(3)	2865(2)
Z	4	4	4	2
D_c/g cm^{-3}	2.052	1.729	1.965	1.832
μ(Mo-Kα)/cm^{-1}	85.90	65.78	74.30	68.87
F(000)	2616	2936	2952	1504
Crystal size/mm	0.32 × 0.25 × 0.16	0.20 × 0.15 × 0.15	0.20 × 0.16 × 0.12	0.22 × 0.15 × 0.12
θ Range for data collection/°	1.86–25.02	1.75–25.09	1.78–25.07	1.76–25.12
h_{min}, h_{max}	−17, 22	−14, 11	−32, 33	−12, 10
k_{min}, k_{max}	−15, 15	−22, 23	−15, 19	−14, 14
l_{min}, l_{max}	−19, 21	−28, 26	−10, 8	−22, 22
Reflections collected	14 909	23 134	15 657	11 444
Unique reflections	6403	8752	7347	7732
R_{int}	0.090	0.0802	0.0620	0.0473
Data, parameters in the refinement	6403, 480	8752, 553	7347, 555	7732, 571
Final $R1$, $wR2$ indices	0.0655 (0.0500)	0.0736 (0.0502)	0.0417 (0.0321)	0.0699 (0.0407)
	0.1212 (0.1188)	0.1318 (0.1291)	0.0851 (0.0838)	0.1102 (0.1067)
Largest difference peak and hole/e Å^{-3}	3.670, −2.030	3.658, −1.097	1.066, −1.519	2.016, −1.226

$R1 = \Sigma(F_o - F_c)/\Sigma(F_o)$; $wR2 = [\Sigma[w(F_o^2 - F_c^2)^2/\Sigma w(F_o^2)^2]^{\frac{1}{2}}$; $w = 1/[\sigma^2(F_o^2) + (aP)^2]$. where $P = [(F_o^2) + 2F_c^2]/3$ with $a = 0.0563$ (**3**), 0.0453 (**4**), 0.0269 (**6**) and 0.0248 (**7**). The $R1$ and $wR2$ values are for all unique data; those calculated for data with $I > 2\sigma(I)$ are given in parentheses.

chromatographic work-up gave **7** (0.007 g, 28%) and **8** (0.004 g, 16%).

X-Ray crystallography

Crystals of complexes **3**, **4**, **6** and **7** were obtained as described above. All measurements were made on a Delft Instruments FAST TV area-detector diffractometer positioned at the window of a rotating-anode generator, using Mo-Kα radiation (λ = 0.710 69 Å) in a manner described previously.[30] In all cases the unit-cell parameters were obtained by least-squares refinement of the diffractometer angles for 250 reflections. The crystallographic data and the data collection and refinement details are presented in Table 5.

All data sets were corrected for absorption using DIFABS.[31] The structures were solved by direct methods (SHELX 86),[32] developed *via* difference syntheses, and refined on F^2 by full-matrix least squares (SHELXL 93)[33] using all unique data with intensities greater than 0. In all cases the non-hydrogen atoms were anisotropic, and the hydrogen atoms belonging to the C_6H_5 and CH_2 groups included in calculated positions (riding model). The P–H hydrogens in **3** and **6** were also allowed to ride on the parent atoms with P–H distance constrained at 1.44(1) Å. In all cases, the phenyl rings were refined as idealized hexagons with C–C distance 1.390 Å and C–C–C angle 120.0°. Crystals of **4** contained a solvate water molecule disordered between two positions in the lattice; similarly compound **7** contained a molecule of CH_2Cl_2 solvate disordered between two positions. Difference maps did not show up the terminal hydride in **4**; however, all the bridging hydrides [H(13) in **4** and H(13) and H(23) in **7**] were located but not refined. The terminal hydride and the hydrogen atoms belonging to the water solvate in **4** were ignored. The determination of the correct absolute structure in the case of **6** was indicated by the final value 0.043(11) of the Flack parameter[34] in SHELXL 93. Final R values are given in Table 5. Sources of scattering factors are as in ref. 33. The molecular diagrams were drawn using SNOOPI.[35]

CCDC reference number 186/887.

See http://www.rsc.org/suppdata/dt/1998/1097/ for crystallographic files in .cif format.

Acknowledgements

This work was supported by the Fonds der Chemischen Industrie and by the Commission for the European Communities. S. E. K. gratefully acknowledges the Alexander von Humboldt Foundation for a fellowship and Royal Society of Chemistry for partial support. M. B. H. and K. M. A. M. acknowledge the EPSRC for the support of the X-ray facilities at Cardiff.

References

1 A. J. Deeming, S. Donovan-Mtunzi and S. E. Kabir, *J. Organomet. Chem.*, 1984, **276**, C65; 1987, **333**, 253.
2 A. J. Deeming, S. Donovan-Mtunzi, K. I. Hardcastle, S. E. Kabir, K. Henrick and M. McPartlin, *J. Chem. Soc.*, *Dalton Trans.*, 1988, 529; A. J. Deeming, K. I. Hardcastle and S. E. Kabir, *J. Chem. Soc.*, *Dalton Trans.*, 1988, 827.
3 A. J. Deeming and S. E. Kabir, *J. Organomet. Chem.*, 1988, **340**, 359.
4 S. E. Kabir, A. Miah, L. Nesa, K. Uddin, K. I. Hardcastle, E. Rosenberg and A. J. Deeming, *J. Organomet. Chem.*, 1995, **492**, 41.
5 S. R. Hodge, B. F. G. Johnson, J. Lewis and P. R. Raithby, *J. Chem. Soc.*, *Dalton Trans.*, 1987, 931.
6 B. F. G. Johnson, J. Lewis, M. Manari, D. Braga, F. Grepioni and C. Gradella, *J. Chem. Soc.*, *Dalton Trans.*, 1990, 2863.
7 J. A. Clucas, D. F. Foster, M. M. Harding and A. K. Smith, *J. Chem. Soc.*, *Chem. Commun.*, 1984, 949.
8 J. A. Clucas, M. M. Harding and A. K. Smith, *J. Chem. Soc.*, *Chem. Commun.*, 1985, 2080.
9 J. A. Clucas, P. A. Dolby, M. M. Harding and A. K. Smith, *J. Chem. Soc.*, *Chem. Commun.*, 1987, 1829.
10 M. M. Harding, B. Kariuki, A. J. Mathews, A. K. Smith and P. Braunstein, *J. Chem. Soc.*, *Dalton Trans.*, 1994, 33.
11 M. P. Brown, P. A. Dolby, M. M. Harding, A. J. Mathews and A. K. Smith, *J. Chem. Soc.*, *Dalton Trans.*, 1993, 1671.

12 D. F. Foster, J. H. Harrison, B. S. Nicholls and A. K. Smith, *J. Organomet. Chem.*, 1985, **295**, 99.
13 S. Cartwright, J. A. Clucas, R. H. Dawson, D. F. Foster, M. M. Harding and A. K. Smith, *J. Organomet. Chem.*, 1986, **302**, 403.
14 K. A. Azam, S. E. Kabir, A. Miah, M. W. Day, K. I. Hardcastle, E. Rosenberg and A. J. Deeming, *J. Organomet. Chem.*, 1992, **435**, 157.
15 J. Powell, E. Fuchs, M. R. Gregg, J. Phillips and M. V. R. Stainer, *Organometallics*, 1990, **9**, 387 and refs. therein.
16 W. C. Fultz, A. L. Rheingold, P. E. Kreter and D. W. Meek, *Inorg. Chem.*, 1983, **22**, 860; P. Y. Zheng, T. T. Nadasdi and D. W. Meek, *Organometallics*, 1989, **8**, 1393.
17 G. G. Hlatky and R. H. Crabtree, *Coord. Chem. Rev.*, 1985, **65**, 1; D. S. Moore and S. D. Robinson, *Chem. Soc. Rev.*, 1983, 415.
18 F. Iwasaki, M. J. Mays, P. R. Raithby, P. L. Taylor and P. J. Wheattey, *J. Organomet. Chem.*, 1981, **213**, 185.
19 V. D. Patel, A. A. Cherkas, D. Nucciarone, N. J. Taylor and A. J. Carty, *Organometallics*, 1985, **4**, 1792.
20 E. Keller and H. Vahrenkamp, *Chem. Ber.*, 1981, **114**, 1124.
21 J. S. Field, R. J. Haines, M. H. Moore, D. N. Smith and L. M. S. Steer, *Afr. J. Chem.*, 1984, 37.
22 S. A. MacLaughlin, N. J. Taylor and A. J. Carty, *Organometallics*, 1984, **3**, 392.
23 G. Lavigne, N. Lugan and J. J. Bonnet, *Organometallics*, 1982, **1**, 1040.
24 M. R. Churchill and B. G. DeBoer, *Inorg. Chem.*, 1977, **16**, 828.
25 A. W. Coleman, D. F. Jones, P. H. Dixneuf, C. Brission, J. J. Bonnet and G. Lavigne, *Inorg. Chem.*, 1984, **23**, 952.
26 G. Lavigne, N. Lugan and J. J. Bonnet, *Acta Crystallogr.*, *Sect. B*, 1982, **38**, 1911.
27 Y. K. Au, K. K. Cheung and W. T. Wong, *J. Chem. Soc.*, *Dalton Trans.*, 1995, 1047.
28 A. J. Carty, S. A. MacLaughlin and N. J. Taylor, *J. Organomet. Chem.*, 1981, **204**, C27.
29 S. E. Kabir, H. Vahrenkamp, M. B. Hursthouse and K. M. A. Malik, *J. Organomet. Chem.*, 1997, **546/537**, 509.
30 J. A. Darr, S. R. Drake, M. B. Hursthouse and K. M. A. Malik, *Inorg. Chem.*, 1993, **32**, 5704.
31 N. P. C. Walker and D. Stuart, *Acta Crystallogr.*, *Sect. A*, 1983, **39**, 158; adapted for FAST geometry by A. I. Karaulov, University of Wales, 1991.
32 G. M. Sheldrick, *Acta Crystallogr.*, *Sect. A*, 1990, **46**, 467.
33 G. M. Sheldrick, SHELXL 93, program for crystal structure refinement, University of Göttingen, 1993.
34 H. D. Flack, *Acta Crystallogr.*, *Sect. A*, 1983, **39**, 876.
35 K. Davies, SNOOPI, program for crystal structure drawing, University of Oxford, 1983.

Received 4*th December* 1997; *Paper* 7/08733K